Polymer 193 (2020) 122358

Contents lists available at ScienceDirect

Polymer

journal homepage: http://www.elsevier.com/locate/polymer

Segmented polyurethanes containing movable rotaxane units on the main chain: Synthesis, structure, and mechanical properties

Jun Sawada [a], Hiromitsu Sogawa [a,1], Hironori Marubayashi [b,2], Shuichi Nojima [b], Hideyuki Otsuka [b], Ken Nakajima [b], Yosuke Akae [a], Toshikazu Takata [a,*]

[a] Department of Chemical Science and Engineering, Tokyo Institute of Technology, 4259 Nagatsuta, Midori-ku, Yokohama, 226-8503, Japan
[b] Department of Chemical Science and Engineering, Tokyo Institute of Technology, 2-12-1 O-okayama, Meguro-ku, Tokyo, 152-8552, Japan

ARTICLE INFO

Keywords:
Rotaxane
Segmented polyurethane
Thermoplastic elastomer

ABSTRACT

In this study, segmented polyurethanes (SPUs), including those with rotaxane structures, were synthesized in high yields (>83%) using a [2]rotaxane diol that has a hydroxy group in each wheel and axle component. The traditional prepolymer method was applied to introduce rotaxane structures at different locations in the soft segment and at the boundary between soft and hard segments. The mechanical properties of the formed SPUs were evaluated via tensile tests, and we determined that the introduction of an appropriate amount of rotaxane structure improved their extensibility, toughness, and stress-relaxing properties. Differential scanning calorimetry (DSC), attenuated total reflection Fourier transform infrared spectroscopy (ATR-FT-IR), and synchrotron X-ray measurements revealed that the phase-separated structures of the SPUs were almost independent of the amount of rotaxane. The highly movable rotaxane scaffold was even effective for toughening the SPU, which is a physically cross-linked network, without changing their phase-separated structures.

1. Introduction

Rotaxane cross-linked polymers (RCPs), which have rotaxane structures at cross-link points, can disperse applied stress owing to the movability of polymer chains at the cross-link points. Therefore, RCPs have remarkable properties, such as excellent toughness, compared with typical cross-linked polymers. Recently, many researchers have developed various types of RCPs from a fundamental scientific and industrial perspective [1–22]. Meanwhile, polyurethanes (PUs), which are mostly synthesized via the polyaddition reaction with α,ω-diols and diisocyanates, are widely utilized as engineering materials for many applications because the functionalization of PUs can be easily achieved by choosing appropriate monomers [23–27]. In particular, segmented polyurethanes (SPUs) form physically cross-linked networks and exhibit good processability, moldability, and recyclability compared with network polymers that have a permanent covalent cross-links. Recently, there have been few reports on PU-based network polymers with rotaxane structures at the cross-link points. These were first established by Gibson's group in 1997. They synthesized target polymers by the polyaddition of 4,4′-methylenebis(*p*-phenyl isocyanate) (MDI), tetraethylene glycol (TEG), and crown ether that has two hydroxy groups [28]. The topological cross-link points were generated by forming a pseudorotaxane complex comprising a crown ether threaded OH-terminated polymer chain during the reaction. They also prepared SPUs having rotaxane scaffold in the hard segment, and found that the yielding behavior was only observed in the presence of macrocycles by tensile tests [29]. Meanwhile, Sagara's group reported the synthesis and mechanochromic behavior of SPUs that have rotaxane structures on their polymer backbones [30]. They found that the mechanical properties of the formed SPUs were almost the same either in the presence or absence of the rotaxane unit because the amount of rotaxane was limited (<0.4 wt%) for clear observation of the mechanochromic fluorescence in their system. Moreover, Murakami and coworkers reported that a rotaxane-connected SPU showed 1.5 times larger fracture strain and energy than a crown ether-threaded SPU, which was the control SPU without the rotaxane structure at the cross-link points [31]. Although an

* Corresponding author.
E-mail address: ttakata@polymer.titech.ac.jp (T. Takata).
[1] Present address: Biomacromolecules Research Team, RIKEN Center for Sustainable Resource Science, 2–1, Hirosawa, Wako-shi, Saitama, 351–0198, Japan (H.S.).
[2] Present address: Institute of Multidisciplinary Research for Advanced Materials, Tohoku University, 2-1-1 Katahira, Aoba-ku, Sendai, Miyagi 980–8577, Japan (H. M.).

https://doi.org/10.1016/j.polymer.2020.122358
Received 22 January 2020; Received in revised form 3 March 2020; Accepted 7 March 2020
Available online 8 March 2020

enhancement in the toughness occurred upon the incorporation of rotaxane scaffolds into the SPUs, they mentioned that the rotaxane structure did not enhance the toughness effectively because the mobility of their inserted rotaxanes was low owing to the strong interaction of the *sec*-ammonium site with the crown ether. Based on this knowledge, it is still challenging to develop a proper synthesis method for SPUs toughened by the rotaxane structure. Broadening the usability of rotaxane cross-linking to physical cross-linked networks has a considerable potential to develop RCPs with novel function, such as recyclability. In this study, to synthesize SPUs that are toughened by the incorporated rotaxane structures, highly movable [2]rotaxane diol with a hydroxy group in each axle and wheel component without strong interactions was designed. This [2]rotaxane scaffold was used in the prepolymer method with poly(tetramethylene ether glycol) (PTMG), 1,4-butanediol (BDO), and hexamethylene diisocyanate (HDI) to produce SPUs with rotaxane structures in their main chain. SPU-based elastomeric films were prepared by the solvent cast method and characterized by several measurements to clarify the effect of the rotaxane structures on the physical properties and phase-separated structures of the SPUs.

2. Experimental

2.1. Materials

Dichloromethane (DCM) was washed with water and dried with $MgSO_4$ and then 4A molecular sieves (Wako: FUJIFILM Wako Chemicals CO., LTD.) before use. Super dehydrated *N,N*-dimethylacetamide (DMAc) was purchased from Wako and used as received. HDI was distilled from CaH_2 before use. PTMG (M_n: 1400) was purchased from Aldrich and dried at 80 °C *in vacuo* overnight. Dibutyltin dilaurate (DBTDL) was dried with 4A molecular sieves before use. BDO was distilled from CaH_2 before use and used as a 1.0 M DMAc solution. Other commercially available reagents and solvents were used as received.

2.2. Instruments

^1H (500 MHz) and ^{13}C (125 MHz) nuclear magnetic resonance (NMR) spectra were recorded on a Bruker AVANCE III HD500 spectrometer, and $CDCl_3$, DMSO-d_6, and THF-d_8 were used as the solvents. It was calibrated using residual undeuterated tetramethylsilane and the solvent as the internal standard. Attenuated total reflection Fourier transform infrared spectroscopy (ATR-FT-IR) was performed on a JASCO FT/IR-6200 spectrometer. High-resolution FAB-MS and ESI-TOF-MS were obtained on a JEOL JMS-700 and a Bruker Daltonics micrOTOF II, respectively, at the Center for Advanced Material Analysis, Tokyo Institute of Technology upon request. Size exclusion chromatography (SEC) was performed at 30 °C in dimethylformamide (DMF) (5 mM LiBr, 0.85 mL/min) using a JASCO PU-2080 system equipped with a set of TOSOH TSKgel G2500H and G4000H columns. The number average molecular weight (M_n), weight average molecular weight (M_w), and polydispersity index (M_w/M_n) of the polymers were calculated based on a polystyrene calibration. Preparative SEC was performed using a LaboACE LC-5060 instrument from Japan Analytical Industry Co., Inc. with a set of JAIGEL-2HR and JAIGEL-2.5HR columns. Thermogravimetric analysis (TGA) was performed on a Shimadzu TGA-50 instrument under N_2 atmosphere (flow rate 50 mL/min) to determine the 5% and 10% weight decomposition temperatures, T_{d5} and T_{d10}, at which the polymers lose 5% and 10% of their weight, respectively. The sample was first heated at a rate of 10 °C/min and kept at 100 °C for 30 min to remove the remaining solvents. Afterwards, the sample was heated again at the same heating rate (10 °C/min) until 180 °C. The glass transition temperatures (T_g) of the polymers were determined by differential scanning calorimetry (DSC) using a Shimadzu DSC-60 instrument in N_2 atmosphere (flow rate 50 mL/min) with liquid N_2 as the refrigerant. The DSC heating rate was 20 °C/min. Simultaneous synchrotron small- and waide-angle X-ray scattering (SAXS and WAXS) measurements were performed at the beam line BL-6A ($\lambda = 0.1500$ nm) of the Photon Factory in KEK (Tsukuba, Japan). Two-dimensional SAXS and WAXS patterns were detected using PILATUS3 1M and 100K (DECTRIS Ltd.), respectively. Samples were kept at constant temperatures (25, 40, 80, and 140 °C) during the measurements. A series of X-ray structure analyses were performed using handmade software [32,33].

2.3. Synthesis

2.3.1. Synthesis of [2]rotaxane diol (6)

A mixture of axle component **1** (2.6 g, 3.7 mmol) and wheel component **2** (2.5 g, 3.2 mmol) in dry DCM (10 mL) was sonicated at r.t. until the solution became transparent to afford a solution of pseudo[2]rotaxane **3**. To a stock solution of **3**, a small amount of dibutyltin dilaurate (DBTDL) and 3,5-dimethylphenyl isocyanate (0.93 g, 6.3 mmol) were added, and stirred for 8 h at r.t. to obtain [2]rotaxane **4** without purification. Then, methanol was added to the mixture to quench the excess isocyanate. After evaporation, the residue was diluted again with dry THF (10 mL). To a solution of **4** in THF, triethylamine (9.9 g, 98 mmol) and acetic anhydride (4.0 g, 39 mmol) were added in order and stirred for 2 days at r.t. The crude product was evaporated and then diluted with EtOAc. The solution was washed with sat. NH_4Cl aq., sat. $NaHCO_3$ aq., and brine, and then it was purified by column chromatography, eluting with DCM/EtOAc = 10/1 (v/v) to produce neutral [2]rotaxane **5** (4.2 g). Subsequently, **5** (4.2 g) was dissolved in dry THF and mixed with 1.0 M tetrabutyl-ammonium fluoride in THF (9.2 mL) and stirred it for 8 h at r.t. The crude was evaporated and then diluted with EtOAc. The solution was washed with sat. NH_4Cl aq. and brine, and then it was purified by column chromatography by eluting with DCM/EtOAc = 1/3 → EtOAc → EtOAc/MeOH = 30/1 (v/v) and preparative SEC eluting with $CHCl_3$ to produce a white solid, [2]rotaxane diol **6** (1.8 g, 1.7 mmol, 44% in total yield).

6 (white solid): ^1H NMR (500 MHz, $CDCl_3$, 298 K) δ 8.37 (s, 0.5H), 8.31 (s, 0.5H), 7.16 (s, 2H), 6.91–6.78 (m, 9H), 6.51 (s, 1H), 4.62–4.58 (m, 2H), 4.46 (s, 1H), 4.40 (s, 1H), 4.36–4.30 (m, 2H), 4.22–4.05 (m, 8H), 3.97–3.78 (m, 12H), 3.59–3.56 (m, 8H), 3.33 (t, $J = 8$ Hz, 1H), 3.17 (t, $J = 8$ Hz, 1H), 2.27 (d, $J = 12$ Hz, 6H), 2.16 (s, 1.5H), 2.10 (s, 1.5H), 2.09 (s, 6H), 1.58–1.47 (m, 2H), 1.47–1.38 (m, 2H), 1.28–0.92 (m, 16H) ppm; ^{13}C NMR (125 MHz, $CDCl_3$, 298 K) δ 170.98, 170.55, 154.69, 154.50, 154.08, 148.51, 148.39, 147.94, 139.72, 139.64, 138.00, 133.45, 133.25, 132.23, 131.39, 130.81, 128.46, 126.60, 123.31, 123.23, 120.68, 119.16, 115.81, 111.91, 111.60, 111.02, 73.13, 73.05, 69.64, 68.14, 68.07, 67.98, 65.21, 64.80, 62.30, 51.33, 47.87, 47.42, 45.96, 29.92, 29.60, 29.51, 29.45, 29.38, 28.98, 28.30, 27.49, 27.00, 26.84, 25.77, 21.91, 21.51, 21.30, 16.41, 16.34 ppm; FAB-MS (*m/z*): calcd for $C_{59}H_{86}N_2O_{14}Na^+$, 1069.5971; found, 1069.5962.

2.3.2. Synthesis of *SPU*

Typical procedure for method A: A mixture of HDI (0.34 g, 2.0 mmol), PTMG (1.4 g, 0.98 mmol), and [2]rotaxane diol **6** (26 mg, 25 μmol) in dry DMAc (10 mL) was degassed by sonication under reduced pressure and purged with Ar gas. To the solution, DBTDL (1 drop) was added, and it was stirred for 4.5 h at 60 °C. Then, to the reaction mixture, BDO solution was added (1.0 mL, 1.0 mmol), and it was stirred for 6 h at 60 °C. Then, to the mixture, methanol (5.0 mL) was added as the quencher of isocyanate, and it was dropped into water (0.20 L), and placed in the refrigerator to produce a white solid. The resulting polymer was filtered and dried in a vacuum oven at 80 °C for 0.5 day to afford **SPU_2.5a** (1.78 g) in a 96% yield. **SPU_5.0a** (1.53 g) was also prepared in a similar manner in an 83% yield.

Typical procedure for method B: A mixture of HDI (0.34 g, 2.0 mmol) and PTMG (1.4 g, 0.98 mmol) in dry DMAc (10 mL) was degassed by sonication under reduced pressure and purged with Ar gas. To the solution, DBTDL (1 drop) was added, and it was stirred for 4.5 h at 60 °C. Then, to the reaction mixture, a BDO-**6** mixed solution (1.0 mL) was added, which was pre-prepared by dissolving [2]rotaxane diol **6** (26 mg,

25 μmol) in BDO solution (1.0 mL, 1.0 mmol), and it was stirred for 6 h at 60 °C. To the mixture, methanol (5.0 mL) was added as the quencher of isocyanate, it was dropped into water (0.20 L) and then placed in the refrigerator to produce a white solid. The resulting polymer was filtered and dried in a vacuum oven at 80 °C for 0.5 day to afford **SPU_2.5b** (1.69 g) in a 91% yield. **SPU_5.0b** (1.77 g) was prepared in a similar manner in a 95% yield.

3. Results and discussion

3.1. Synthesis of SPUs and their elastomeric films

The [2]rotaxane diol (**6**) containing a hydroxy group on each axle and wheel component was synthesized according to Scheme 1. The chain length of [2]rotaxane diol should be important because it is closely related to the movable range of the rotaxane structure. In fact, we have previously evaluated the effect of the chain length of [2]rotaxane crosslinkers in vinyl-polymer system, and found that the formed RCPs showed superior mechanical performance with the use of [2]rotaxane crosslinkers having C6 and C12 alkyl chains compared to macromolecular [2]rotaxane crosslinkers, which have longer chain lengths [13,20,21]. Based on these results, in this study, we decided to synthesize [2]rotaxane diol having C12 alkyl chain. The axle component with a *sec*-ammonium site, one hydroxy group, and one tri-*iso*-propylsilyl (TIPS)-protected hydroxy group (**1**) was synthesized in six steps from 4-hydroxy-3,5-dimethylbenzealdehyde (see ESI for details). Crown ether with a TIPS-protected hydroxy group (**2**) was also prepared according to our previous report [34]. A mixture of **1** and **2** in DCM was sonicated until completely dissolved for the formation of pseudo[2]rotaxane intermediate **3**. It was further treated with a bulky end-cap agent, i.e., 3,5-dimethylphenyl isocyanate, to afford [2]rotaxane **4**. Subsequently, *N*-acetylation of the *sec*-ammonium site and deprotection of the hydroxy group was conducted to produce **6** in a 44% total yield. The chemical structure of **6** was confirmed by ^{1}H NMR (Fig. S2), and its high purity (>99%) was determined by liquid chromatography (LC). Then, target SPUs were synthesized by the prepolymer method using PTMG (M_n: 1400), HDI, and BDO as the polymeric diol, diisocyanate, and chain extender, respectively (Scheme 2). Son reported that SPUs made from PTMG soft segment with molecular weights below 1400 had phase mixing between hard and soft segments [35]. Meanwhile, we suspect that the adequate evaluation of the effect of [2]rotaxane structure becomes difficult with the use of PTMG with higher molecular weight chain as the mechanical properties of formed SPUs are mainly dominated by the effect of PTMG chain. Thus, in this study, the chain length of PTMG was fixed at 1400. **6** was added in two different steps to introduce the rotaxane structure at different locations on the polymer chains. Namely, **6** was used for prepolymer synthesis with PTMG via method A and for the chain extender with BDO via method B, respectively. The rotaxane structure was expected to be located in the soft segment via method A, while in the hard segment via method B. The feed ratios of **6** were 2.5 and 5.0 mol% against PTMG via method A and against BDO via method B while keeping the ratio of (PTMG + **6**)/HDI/(BDO + **6**) as 1/2/1 in each case. SPUs synthesized via method A were named as **SPU_xa**, whereas SPUs synthesized via method B were named as **SPU_xb**. The SPU (**SPU_0**) without the rotaxane structure (x = 0) was also synthesized as a control. Note that the formed SPUs did not contain a rotaxane structure at the cross-link points of network structures as in our reported vinyl polymer-based RCPs [4,17,20,21]. The results are summarized in Table 1. Rotaxane diol **6** reacted with HDI well and afforded the corresponding SPUs, whose molecular weights and PDI were almost the same based on SEC measurements in more than an 80% yield. Subsequently, the obtained SPUs were dissolved in THF, placed into a PTFE container, and dried first under ambient atmosphere until THF evaporated and then *in vacuo* at 80 °C for 12 h to produce SPU elastomeric films whose thickness was approximately 250 μm. The ratios of **6**/HDI of resulting films were consistent with the feed ratios of **6** according to the ^{1}H NMR spectra (Fig. S3). Additionally, M_w were similar among all SPU elastomeric films including **SPU_0**, indicating that the effect of molecular weights on the mechanical properties should be negligible.

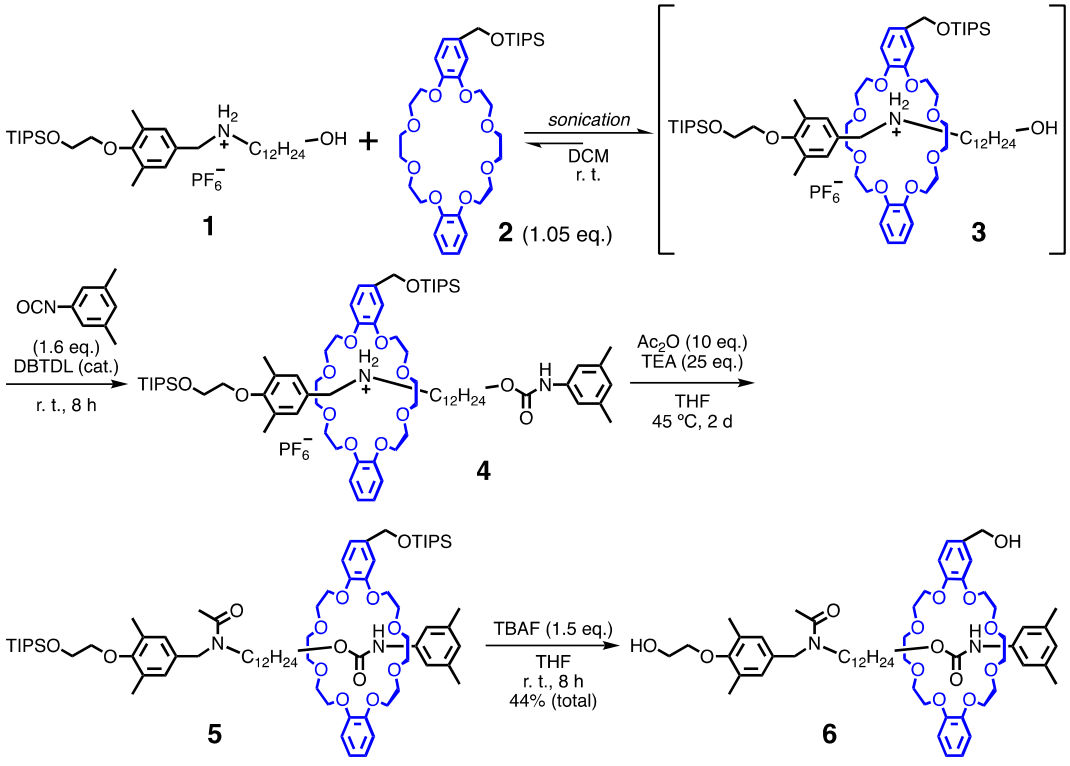

Scheme 1. Synthesis of [2]rotaxane diol **6**.

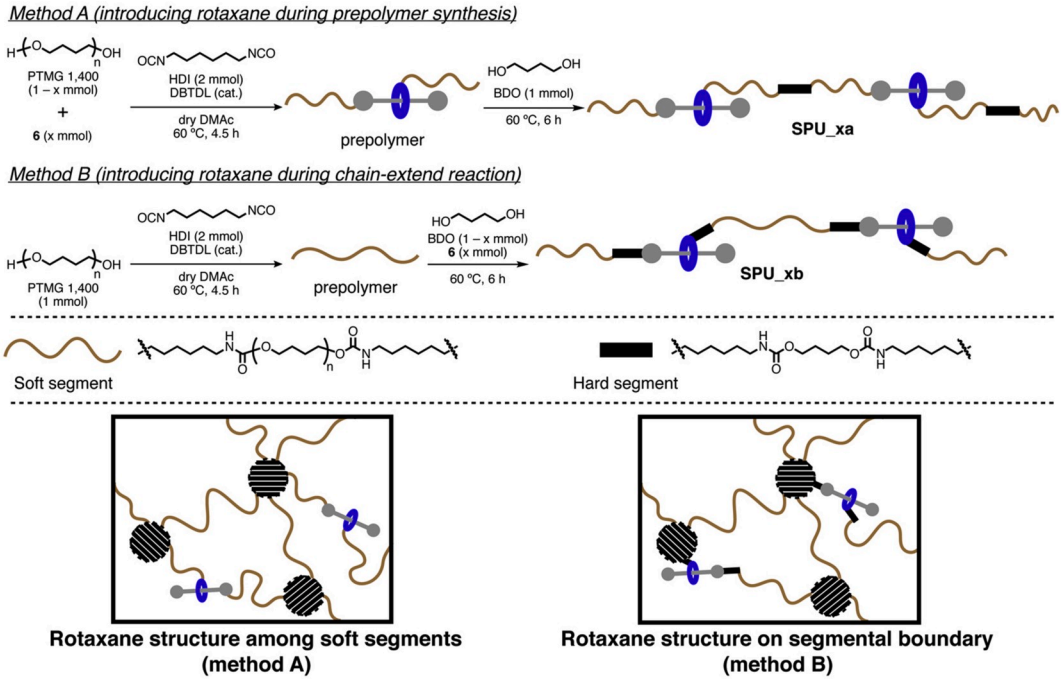

Scheme 2. Schematic illustration of SPUs with the rotaxane structure.

Table 1
Summary of the synthesis of SPUs and the fabrication of their elastomeric films.

Code	Method	Feed ratio of **6**	As prepared SPU			SPU films			
			Yield (%)[a]	M_w (kDa)[b]	PDI[b]	Yield (%)[a]	**6**/HDI[c]	M_w (kDa)[b]	PDI[b]
SPU_5.0a	A	5.0	83	31	1.8	96	2.7	25	1.7
SPU_2.5a	A	2.5	96	34	1.9	97	1.5	29	1.7
SPU_0	–	–	91	24	2.0	97	–	25	1.7
SPU_2.5b	B	2.5	91	28	1.6	94	1.4	30	1.6
SPU_5.0b	B	5.0	95	33	1.9	97	3.0	27	1.7

[a] Calculated by weight after drying *in vacuo*.
[b] Determined by SEC (eluent: DMF; polystyrene standards; detected by RI).
[c] Calculated by ^{1}H NMR (Fig. S3). The amount of HDI was fixed at 2 mmol.

3.1.1. Mechanical properties of the SPU elastomeric films

To evaluate the mechanical properties of the SPU elastomeric films, tensile tests were conducted (Fig. 1). As a result, **SPU_2.5a** and **SPU_2.5b** showed larger fracture strain (100%~) than the control sample, **SPU_0** (64%). Moreover, **SPU_2.5b** had the largest fracture stress (3.5 MPa) and fracture energy (3.2 MJ/m^3), which was twice as large as that of **SPU_0**. The introduction of the highly movable rotaxane structure in the main chain of thermoplastic SPU elastomers would endow them with toughness. Meanwhile, the toughness of **SPU_2.5b** was better than that of **SPU_2.5a** despite having the same rotaxane content. Yoshie and coworkers reported that the efficiency of the stress dispersing moieties increased at the boundary between hard and soft segments of thermoplastic elastomers compared to other positions [36]. Based on their idea, **SPU_2.5b** exhibited a larger toughness than **SPU_2.5a** because the rotaxane structure was located on the boundary in method B, as expected. Meanwhile, the increase in the rotaxane content did not proportionally enhance the toughness because **SPU_5.0a** and **SPU_5.0b** showed weaker mechanical properties compared with **SPU_2.5a** and **SPU_2.5b**. This is likely because the rotaxane structures also worked as a plasticizer. The effect as a plasticizer would surpass the stress dispersing effect with a high rotaxane content, resulting in lowering the mechanical properties. This assumption was supported by the experimental results in which the Young's moduli of **SPU_5.0a** and **SPU_5.0b** were lower than that of **SPU_0**. We further synthesized **SPU_1.5a** and **SPU_1.5b** in a similar manner to other SPUs and evaluated mechanical properties. Briefly, the mechanical performance of **SPU_1.5a** and **SPU_1.5b** was better than **SPU_0**, but worse than **SPU_2.5a** and **SPU_2.5b** (Fig. S4). These results also suggest the incorporation of the rotaxane structure has a potential to toughen the formed SPUs with the threshold value. Next, cycle tensile tests were conducted (Fig. 2). Interestingly, the SPUs with rotaxane structures clearly showed smaller hysteresis energy loss compared with **SPU_0**. In particular, the energy loss of **SPU_2.5b**, which exhibited the largest toughness among all the SPUs, was negligible at the 1st cycle (10% strain) and was reduced almost by half for **SPU_0** at the 3rd cycle (30% strain). These results clearly suggest that the rotaxane structure in the physically cross-linked polymers dispersed the applied stress to prevent breaking of the polymer network. The incorporation of rotaxane structures was effective for not only toughening but also inhibiting energy loss.

3.1.2. Structural characterization of the SPU elastomeric films

To obtain structural information about the SPUs, TGA, DSC, ATR-FT-IR, SAXS, and WAXS measurements were performed. Table 2 summarizes the thermal properties of SPUs. TGA measurements revealed that the introduction of the rotaxane structure into the main chain of the SPUs did not reduce its thermal stability because the 5 wt% and 10 wt% thermal decomposition temperatures (T_{d5} and T_{d10}) of all SPUs were about the same. The same tendency was determined from the DSC

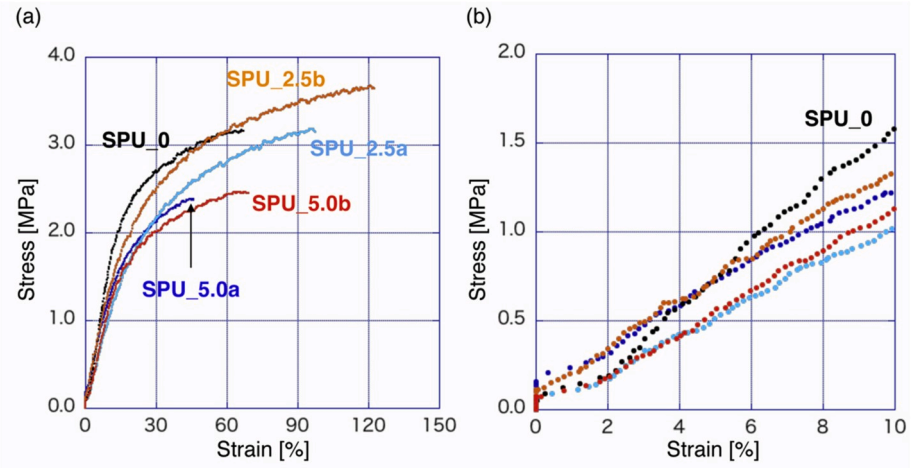

(c)

SPU	Film thickness [μm]	Young's Modulus [MPa]	Fracture Strain [%]	Fracture Stress [MPa]	Fracture Energy [MJ/m³]
SPU_5.0a	340 ± 26	12 ± 0.9	45 ± 1.3	2.4 ± 0.05	0.76 ± 0.03
SPU_2.5a	270 ± 27	10 ± 0.7	100 ± 9.9	3.2 ± 0.14	2.4 ± 0.34
SPU_0	260 ± 9	17 ± 1.0	64 ± 2.1	3.1 ± 0.13	1.6 ± 0.08
SPU_2.5b	240 ± 17	12 ± 2.2	120 ± 6.8	3.5 ± 0.13	3.2 ± 0.23
SPU_5.0b	260 ± 28	13 ± 1.1	62 ± 3.7	2.4 ± 0.07	1.2 ± 0.11

Fig. 1. Stress–strain (S–S) curves of SPUs (a) in the full range and (b) in the expanded range and (c) summary of the mechanical properties of SPUs.

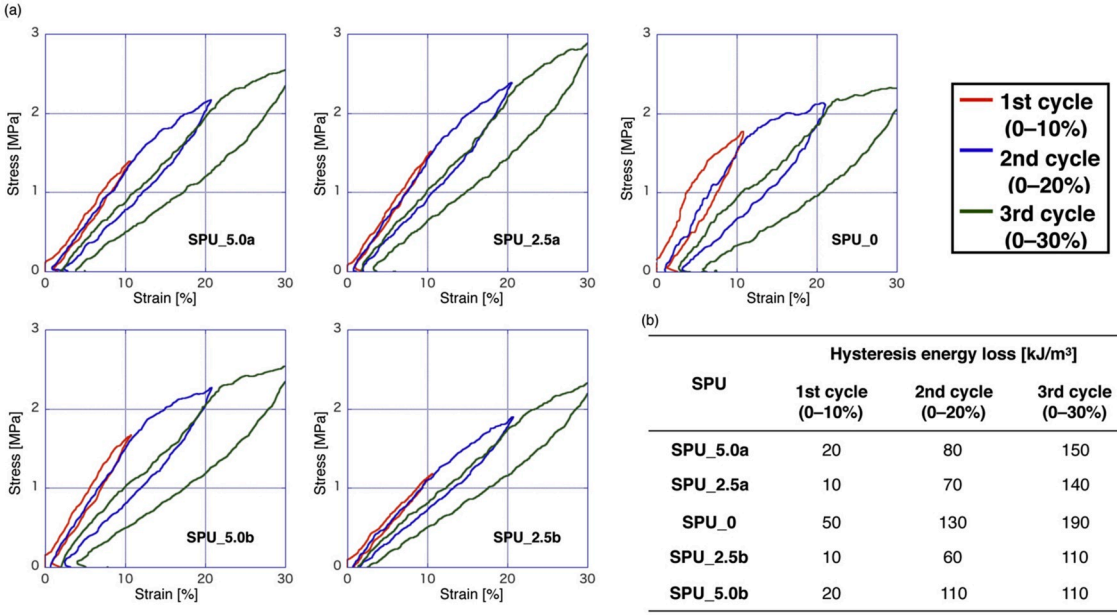

(b)

SPU	Hysteresis energy loss [kJ/m³]		
	1st cycle (0–10%)	2nd cycle (0–20%)	3rd cycle (0–30%)
SPU_5.0a	20	80	150
SPU_2.5a	10	70	140
SPU_0	50	130	190
SPU_2.5b	10	60	110
SPU_5.0b	20	110	110

Fig. 2. Cycle tensile tests of the SPUs: (a) S–S curves and (b) summary of the hysteresis energy loss.

measurements (For DSC charts, see Fig. S5). Specifically, all SPUs showed one glass transition (T_g) and two melting temperatures (T_m) for almost the same temperature ranges. According to a reference [37], the T_g and lower T_m originated from PTMG, which was applied to the soft segment. On the other hands, a higher T_m was estimated to have originated from the collapse of the crystallized structure of the hard segment, which was stabilized by intermolecular hydrogen bonds. Moreover, the crystallinity percentages of SPUs were likely the same because enthalpy values (ΔH_m) of T_m were also the same. Meanwhile, the presence of hydrogen bonds was evaluated by ATR-FT-IR spectra (Fig. S6). Two main regions, which showed N–H absorption and C═O stretching, were focused in Fig. 3. The hydrogen-bonded N–H absorption peak centered at 3320 cm^{-1} and C═O stretching peak at approximately 1705 cm^{-1} were clearly observed for all SPUs [38,39]. Moreover, the relative ratio

Table 2
Thermal properties of SPUs.

Code	TGA		DSC				
	T_{d5} (°C)	T_{d10} (°C)	T_g (°C)	T_{m_s} (°C)[a]	ΔH_{m_s} (J/g)[a]	T_{m_h} (°C)[b]	ΔH_{m_h} (J/g)[b]
SPU_5.0a	303	326	−79	16	22	90	10
SPU_2.5a	298	320	−80	11	21	87	5.2
SPU_0	306	329	−81	11	27	86	9.0
SPU_2.5b	307	327	−80	16	23	86	8.7
SPU_5.0b	305	330	−79	16	23	98	11
PTMG	270	286	–[c]	24	84	–[c]	–[c]

[a] Originated from the soft segment.
[b] Originated from the hard segment.
[c] Not detected.

between the hydrogen-bonded C═O stretching peak and free C═O centered at 1720 cm^{-1} did not change considerably. These results suggest that the microphase-separated structure did not change considerably in the presence of the rotaxane structures. Besides, simultaneous SAXS and WAXS measurements were conducted at various temperatures. The samples were annealed at 80 °C, which was slightly lower than T_{m_h}, for 12 h before the measurements, and the effect of this annealing time (0, 12, and 240 h) on the SAXS and WAXS results was confirmed to be negligible. In the SAXS profiles, broad scattering peaks due to the microphase-separated structure of the hard and soft domains [40] were observed at 25 °C and became sharper at 80 °C (Fig. 4a). A further increase in the temperature up to 140 °C resulted in a drastic decrease in the peak intensity and the disappearance of the peaks for **SPU_0** and **SPU_5.0b** (very weak peaks were still observed for **SPU_2.5a**, **SPU_5.0a**, and **SPU_2.5b**). The domain spacing ($d = 2\pi/q$, where $q = 4\pi\sin\theta/\lambda$) was determined to be approximately 14 nm at 25 °C and increased upon increasing the temperature (Fig. 4b). In the WAXS profiles (Fig. 4c), all samples exhibited weak peaks and shoulders at 25 and 40 °C, which could be attributed to (020), (021), and (110) of the PTMG crystal [40,41]. Additionally, the peak-top (T_{m_s}) and end-set of the DSC melting peak for the soft segments were 11–16 and ca. 40 °C, respectively (Fig. S5). Thus, these results showed that relatively thick crystallites of soft segments with PTMG blocks existed at 25 °C and melting proceeded but thicker crystallites still survived even upon increasing the temperature up to 40 °C. In contrast, the samples showed an amorphous halo at 80 ($<T_{m\_h}$) and 140 °C ($>T_{m\_h}$). Fig. 4d summarizes the crystallinity of the soft domains in the SPUs. The crystallinity was calculated for the entire sample. A gradual decrease in the crystallinity upon increasing the temperature was clearly observed, indicating melting of microcrystallites in the soft domains proceeded with increasing temperature. In all SPUs, SAXS peaks were still detected at 80 °C even though the WAXS crystallinity became zero or approximately zero at this temperature. Thus, a microphase-separated structure was formed in all SPUs. This microphase-separated structure was composed of partially crystallized soft domains and hydrogen-bonded hard domains in all SPUs at room temperature, which is the condition in which tensile tests were conducted. Namely, the incorporation of the rotaxane structure did not affect the microphase-separated or the crystal structures of the SPUs with at least these rotaxane contents (approximately 1.5 wt% in **SPU_2.5a** and **SPU_2.5b**, whereas 3.0 wt% in **SPU_5.0a** and **SPU_5.0b**). Therefore, the difference in the mechanical properties should have originated from the highly movable characteristics of the rotaxane scaffold.

3.1.3. *Recyclability of the SPU elastomeric films*

Finally, the recyclability of the SPU films was evaluated (Fig. 5). After tensile deformation, **SPU_2.5b** was dissolved in THF again and reconstructed into a film, following the same preparation procedure. As a result, there was no considerable difference in the molecular weights and S–S curves between the 1st casting and the reconstructed film. These results suggest that neither irreversible breaking of the polymer backbones nor the decomposition of the rotaxane structures took place when the film was fractured. The reversible dissociation of hydrogen bonds was expected, as is typical in SPUs. Thus, we successfully prepared recyclable SPUs that included rotaxane structures.

4. Conclusions

[2]Rotaxane diol with a hydroxy group in each wheel and axle

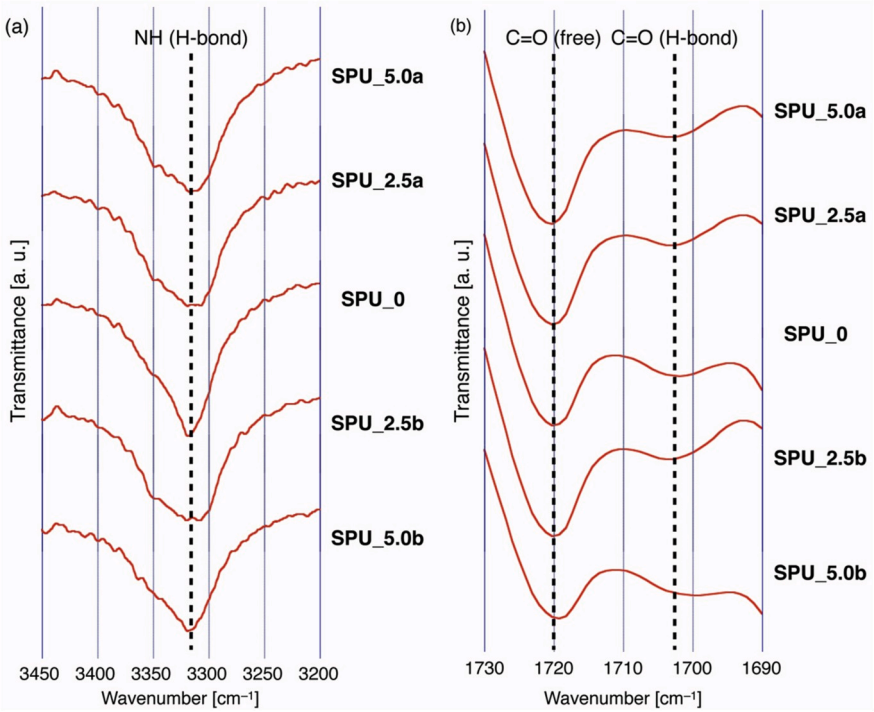

Fig. 3. ATR-FT-IR spectra of the **SPU** films in the ranges of (a) 3450–3200 cm^{-1} and (b) 1730–1690 cm^{-1}.

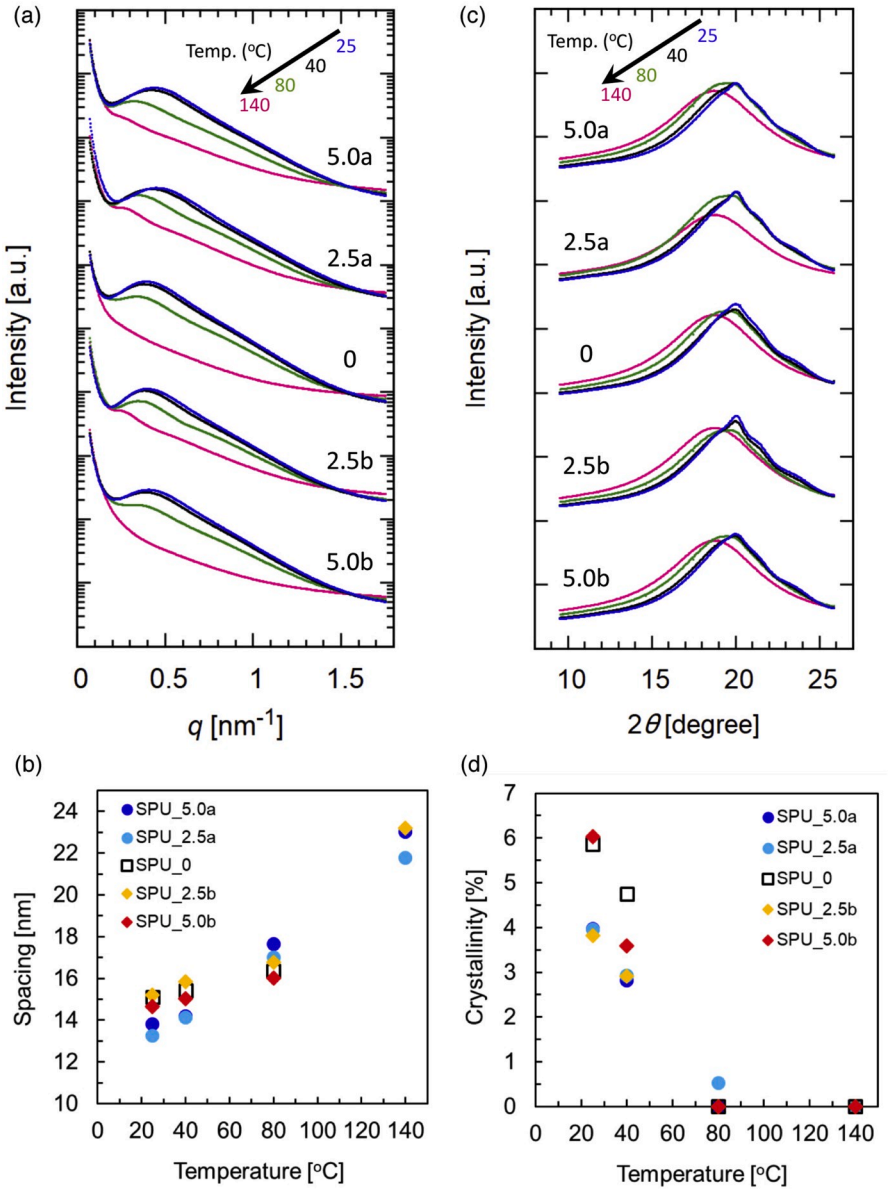

Fig. 4. (a) SAXS profiles, (b) temperature dependence of *d*-spacing in SPUs, (c) WAXS profiles, and (d) temperature dependence of the crystallinity of SPUs.

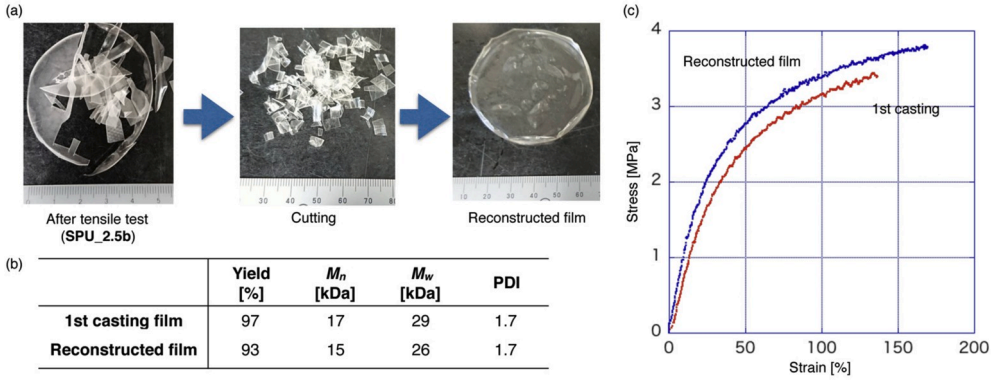

(b)

	Yield [%]	M_n [kDa]	M_w [kDa]	PDI
1st casting film	97	17	29	1.7
Reconstructed film	93	15	26	1.7

Fig. 5. Recyclability of **SPU_2.5b**: (a) Reconstruction protocol of **SPU_2.5b**, (b) molecular weight determined by SEC (eluent: DMF; polystyrene standards; detected by RI), and (c) S–S curves of the as prepared and reconstructed **SPU_2.5b**.

component that did not have any specific interaction was synthesized and used for synthesis of SPUs with a rotaxane structure via a prepolymer method. The SPU-based elastomeric film, which was fabricated with using 2.5 mol% [2]rotaxane diol against BDO as the chain extender (**SPU_2.5b**) showed the best mechanical properties. The fracture strain and energy of **SPU_2.5b** were approximately twice as much as **SPU_0**, which did not contain the rotaxane structure. This revealed that introduction of an appropriate amount of rotaxane structures can enhance the toughness of SPU elastomers. The rotaxane structure in the physically cross-linked polymer could also disperse applied stress, and **SPU_2.5b** was found to possess good recyclability. Further tuning of the chain lengths of [2]rotaxane diol and PTMG is ongoing and will be published elsewhere soon.

Declaration of competing interest

The authors declare that they have no known competing financial interests or personal relationships that could have appeared to influence the work reported in this paper.

CRediT authorship contribution statement

Jun Sawada: Methodology, Investigation, Resources, Writing - original draft, Visualization. **Hiromitsu Sogawa:** Conceptualization, Methodology, Investigation, Writing - original draft, Visualization. **Hironori Marubayashi:** Formal analysis, Investigation, Writing - original draft, Visualization. **Shuichi Nojima:** Writing - review & editing. **Hideyuki Otsuka:** Methodology, Writing - review & editing. **Ken Nakajima:** Resources, Writing - review & editing. **Yosuke Akae:** Resources, Writing - review & editing. **Toshikazu Takata:** Writing - review & editing, Supervision.

Acknowledgements

This research was financially supported by JST CREST Grant Number JPMJCR1522, JSPS KAKENHI Grant Number JP16K17955, and International Polyurethane Technology Foundation. Synchrotron SAXS/WAXS measurements have been performed under the approval of Photon Factory Advisory Committee (Nos. 2018G655 and 2017G084). The authors also would like to thank Enago (www.enago.jp) for the English language review.

Appendix A. Supplementary data

Supplementary data to this article can be found online at https://doi.org/10.1016/j.polymer.2020.122358.

References

[1] Y. Okumura, K. Ito, The polyrotaxane gel: a topological gel by figure-of-eight cross-links, Adv. Mater. 13 (7) (2001) 485–487.
[2] Y. Kohsaka, K. Nakazono, Y. Koyama, S. Asai, T. Takata, Size-Complementary rotaxane cross-linking for the stabilization and degradation of a supramolecular network, Angew. Chem. Int. Ed. 50 (21) (2011) 4872–4875.
[3] M. Ogawa, A. Kawasaki, Y. Koyama, T. Takata, Synthesis and properties of a polyrotaxane network prepared from a Pd-templated bis-macrocycle as a topological cross-linker, Polym. J. 43 (11) (2011) 909–915.
[4] T. Arai, K. Jang, Y. Koyama, S. Asai, T. Takata, Versatile supramolecular cross-linker: a rotaxane cross-linker that directly endows vinyl polymers with movable cross-links, Chem. Eur J. 19 (19) (2013) 5917–5923.
[5] S. Tan, A. Blencowe, K. Ladewig, G.G. Qiao, A novel one-pot approach towards dynamically cross-linked hydrogels, Soft Matter 9 (21) (2013) 5239–5250.
[6] M. Arunachalam, H.W. Gibson, Recent developments in polypseudorotaxanes and polyrotaxanes, Prog. Polym. Sci. 39 (2014) 1043–1073.
[7] A. Bin Imran, K. Esaki, H. Gotoh, T. Seki, K. Ito, Y. Sakai, Y. Takeoka, Extremely stretchable thermosensitive hydrogels by introducing slide-ring polyrotaxane cross-linkers and ionic groups into the polymer network, Nat. Commun. 5 (2014) 5124.
[8] K. Iijima, Y. Kohsaka, Y. Koyama, K. Nakazono, S. Uchida, S. Asai, T. Takata, Stimuli-degradable cross-linked polymers synthesized by radical polymerization using a size-complementary [3]rotaxane cross-linker, Polym. J. 46 (1) (2014) 67–72.
[9] Y. Koyama, Synthesis of topologically crosslinked polymers with rotaxane-crosslinking points, Polym. J. 46 (6) (2014) 315–322.
[10] Y. Noda, Y. Hayashi, K. Ito, From topological gels to slide-ring materials, J. Appl. Polym. Sci. 131 (15) (2014) 40509.
[11] T. Ogoshi, T. Aoki, S. Ueda, Y. Tamura, T.A. Yamagishi, Pillar[5]arene-based nonionic polyrotaxanes and a topological gel prepared from cyclic host liquids, Chem. Commun. 50 (50) (2014) 6607–6609.
[12] M. Inutsuka, K. Inoue, Y. Hayashi, A. Inomata, Y. Sakai, H. Yokoyama, K. Ito, Highly dielectric and flexible polyrotaxane elastomer by introduction of cyano groups, Polymer 59 (2015) 10–15.
[13] J. Sawada, D. Aoki, S. Uchida, H. Otsuka, T. Takata, Synthesis of vinylic macromolecular rotaxane cross-linkers endowing network polymers with toughness, ACS Macro Lett. 4 (5) (2015) 598–601.
[14] J.H. Seo, M. Fushimi, N. Matsui, T. Takagaki, J. Tagami, N. Yui, UV-cleavable polyrotaxane cross-linker for modulating mechanical strength of photocurable resin plastics, ACS Macro Lett. 4 (10) (2015) 1154–1157.
[15] K. Iwaso, Y. Takashima, A. Harada, Fast response dry-type artificial molecular muscles with [c2]daisy chains, Nat. Chem. 8 (6) (2016) 626–633.
[16] S. Hiroshige, T. Kureha, D. Aoki, J. Sawada, D. Aoki, T. Takata, D. Suzuki, formation of tough films by evaporation of water from dispersions of elastomer microspheres crosslinked with rotaxane supramolecules, Chem. Eur J. 23 (35) (2017) 8405–8408.
[17] K. Iijima, D. Aoki, H. Otsuka, T. Takata, Synthesis of rotaxane cross-linked polymers with supramolecular cross-linkers based on γ-CD and PTHF macromonomers: the effect of the macromonomer structure on the polymer properties, Polymer 128 (2017) 392–396.
[18] K. Minato, K. Mayumi, R. Maeda, K. Kato, H. Yokoyama, K. Ito, Mechanical properties of supramolecular elastomers prepared from polymer-grafted polyrotaxane, Polymer 128 (2017) 386–391.
[19] T. Murakami, B.V.K.J. Schmidt, H.R. Brown, C.J. Hawker, Structural versatility in slide-ring gels: influence of Co-threaded cyclodextrin spacers, J. Polym. Sci., Part A: Polym. Chem. 55 (2017) 1156–1165.
[20] J. Sawada, D. Aoki, M. Kuzume, K. Nakazono, H. Otsuka, T. Takata, A vinylic rotaxane cross-linker for toughened network polymers from the radical polymerization of vinyl monomers, Polym. Chem. 8 (2017) 1878–1881.
[21] J. Sawada, D. Aoki, T. Takata, Vinylic rotaxane cross-linker comprising different axle length for the characterization of rotaxane cross-linked polymers, Macromol. Symp. 372 (1) (2017) 115–119.
[22] Y. Akae, H. Sogawa, T. Takata, Cyclodextrin-based [3]Rotaxane-Crosslinked fluorescent polymer: synthesis and de-crosslinking using size complementarity, Angew. Chem. Int. Ed. 57 (45) (2018) 14832–14836.
[23] D.K. Chattopadhyay, K.V.S.N. Raju, Structural engineering of polyurethane coatings for high performance applications, Prog. Polym. Sci. 32 (3) (2007) 352–418.
[24] E. Delebecq, J.-P. Pascault, B. Boutevin, F. Ganachaud, On the versatility of urethane/urea bonds: reversibility, blocked isocyanate, and non-isocyanate polyurethane, Chem. Rev. 113 (1) (2013) 80–118.
[25] K. Imato, T. Kanehara, T. Ohishi, M. Nishihara, H. Yajima, M. Ito, A. Takahara, H. Otsuka, Mechanochromic dynamic covalent elastomers: quantitative stress evaluation and autonomous recovery, ACS Macro Lett. 4 (11) (2015) 1307–1311.
[26] K. Imato, T. Kanehara, S. Nojima, T. Ohishi, Y. Higaki, A. Takahara, H. Otsuka, Repeatable mechanochemical activation of dynamic covalent bonds in thermoplastic elastomers, Chem. Commun. 52 (69) (2016) 10482–10485.
[27] A.V. Menon, G. Madras, S. Bose, The journey of self-healing and shape memory polyurethanes from bench to translational research, Polym. Chem. 10 (32) (2019) 4370–4388.
[28] C.G. Gong, H.W. Gibson, Controlling polymeric topology by polymerization conditions: mechanically linked network and branched poly(urethane rotaxane)s with controllable polydispersity, J. Am. Chem. Soc. 119 (37) (1997) 8585–8591.
[29] D. Loveday, G.L. Wilkes, M.C. Bheda, Y.X. Shen, H.W. Gibson, Structure-property relationships in segmented polyviologen ionene rotaxanes, J. Macromol. Sci., Part A 32 (1) (1995) 1–27.
[30] Y. Sagara, M. Karman, E. Verde-Sesto, K. Matsuo, Y. Kim, N. Tamaoki, C. Weder, Rotaxanes as mechanochromic fluorescent force transducers in polymers, J. Am. Chem. Soc. 140 (2018) 1584–1587.
[31] H. Murakami, R. Nishiide, S. Ohira, A. Ogata, Synthesis of MDI and PCL-diol-based polyurethanes containing [2] and [3]rotaxanes and their properties, Polymer 55 (24) (2014) 6239–6244.
[32] H. Marubayashi, S. Asai, M. Sumita, Complex crystal formation of poly (l-lactide) with solvent molecules, Macromolecules 45 (3) (2012) 1384–1397.
[33] H. Marubayashi, S. Asai, T. Hikima, M. Takata, T. Iwata, Biobased copolymers composed of l-lactic acid and side-chain-substituted lactic acids: synthesis, properties, and solid-state structure, Macromol. Chem. Phys. 214 (22) (2013) 2546–2561.
[34] D. Aoki, S. Uchida, T. Takata, Mechanically linked block/graft copolymers: effective synthesis via functional macromolecular [2]Rotaxanes, ACS Macro Lett. 3 (4) (2014) 324–328.
[35] T.W. Son, D.W. Lee, S.K. Lim, Thermal and phase behavior of polyurethane based on chain extender, 2,2-Bis-[4-(2-hydroxyethoxy)phenyl]propane, Polym. J. 31 (7) (1999) 563–568.
[36] S. Yoshida, H. Ejima, N. Yoshie, Tough elastomers with superior self-recoverability induced by bioinspired multiphase design, Adv. Funct. Mater. 27 (30) (2017) 1701670.
[37] S.H. Jang, J. Lee, J.W. Chung, S.H. Kim, Effects of macromonomeric length of ureidopyrimidinone-induced supramolecular polymers on their crystalline

structure and mechanical/rheological properties, Macromol. Res. 27 (7) (2019) 729–737.
[38] L. Ning, W. De-Ning, Y. Sheng-Kang, Crystallinity and hydrogen bonding of hard segments in segmented poly(urethane urea) copolymers, Polymer 37 (16) (1996) 3577–3583.
[39] A. Pattanayak, S.C. Jana, Thermoplastic polyurethane nanocomposites of reactive silicate clays: effects of soft segments on properties, Polymer 46 (14) (2005) 5183–5193.
[40] J.T. Koberstein, T.P. Russell, Simultaneous SAXS-DSC study of multiple endothermic behavior in polyether-based polyurethane block copolymers, Macromolecules 19 (3) (1986) 714–720.
[41] K. Mitrach, D. Pospiech, L. Häußler, D. Voigt, D. Jehnichen, M. Rätzsch, Thermotropic block copolymers: polyesters with flexible poly (tetramethylene glycol) units in the main chain, Polymer 34 (16) (1993) 3469–3474.